

# InGaN-Based Light-Emitting Diodes with a Cone-Shaped Sidewall Structure Fabricated Through a Crystallographic Wet Etching Process

Chia-Feng Lin,<sup>a,z</sup> Chun-Min Lin,<sup>a</sup> Chung-Chieh Yang,<sup>a</sup> Wei-Kai Wang,<sup>a</sup> Yu-Chieh Huang,<sup>b</sup> Jien-An Chen,<sup>b</sup> and Ray-Hua Horng<sup>b</sup>

<sup>a</sup>Department of Materials Science and Engineering and <sup>b</sup>Institute of Precision Engineering, National Chung Hsing University, Taichung 402, Taiwan

The InGaN-based light-emitting diodes (LEDs) were fabricated through a crystallographic etching process to increase their light extraction efficiency. After the laser scribing and the selective lateral wet etching processes at the LED chip edge region, the stable crystallographic etching planes were formed as the GaN  $\{10\overline{12}\}$  planes and had an including angle with the top GaN (0001) plane measured as  $40.3^{\circ}$ . The AlN buffer layer acted as the sacrificial layer for the lateral wet process with a  $27.5~\mu$ m/h etching rate. The continuous cone-shaped sidewall (CSS) structure of the treated LED has a larger light-scattering area and higher light extraction cones around the LED chips. The LED with the CSS structure around the chip edge region has a higher light output power compared to a conventional LED when measured in LED chip form.

© 2009 The Electrochemical Society. [DOI: 10.1149/1.3118503] All rights reserved.

Manuscript submitted February 3, 2009; revised manuscript received March 9, 2009. Published April 10, 2009.

Gallium nitride materials have attracted considerable interest in the development of optoelectronic devices, such as light-emitting diodes (LEDs) and laser diodes. Consequently, bright blue LEDs require an increase in their internal and external quantum efficiencies. The lower external quantum efficiency of the InGaN-based LEDs is due to a larger refractive index difference between the GaN layer and the surrounding air ( $\Delta n \sim 1.5$ ). Techniques used to increase light extraction have included light output coupling through surface plasmons, corrugated Bragg gratings, and random surface texturing 1-5 to convert waveguided modes into free-space modes. Bottom pattern Al<sub>2</sub>O<sub>3</sub> substrates, top p-type GaN:Mg surface rough processes, <sup>7,8</sup> the forming of photonic crystal structures, <sup>9-12</sup> the periodic deflector embedded structures, <sup>13</sup> and selective oxidization on the mesa sidewall<sup>14</sup> through a photoelectrochemical (PEC) wet oxidation process have been used to increase light-extraction efficiency in InGaN-based LEDs on Al<sub>2</sub>O<sub>3</sub> substrates. Fujii et al. 15 reported that a laser-liftoff technique followed by an anisotropic etching process to roughen the surface (an n-side-up GaN-based LED with a hexagonal "conelike" surface) has been fabricated to increase the extraction efficiency. In addition, research efforts have integrated ZnO nanostructures on GaN light-emitting diodes for enhanced emission efficiency. 16-18 Both the AlInGaP-based LED with the truncated inverted pyramid structures and the GaN-based LEDs with the ATON technique on the SiC substrate 19 for the substrate-shaping process can enhance light-extraction efficiency. Lee et al.<sup>20</sup> reported that experimental results, including photoluminescence and nearand far-field patterns, indicate that the proposed sidewall-deflectorintegrated LED structure enhances the overall surface emission intensity via the proposed mechanism by up to 3.1 times for a sidewall angle of 30°. Kim et al. 21 have reported that GaN-based LEDs with peripheral microhole arrays (PMA-LEDs) have been grown and fabricated on SiO<sub>2</sub> hexagonal pattern masks using selective metallorganic chemical vapor deposition (MOCVD). The light output intensity of the PMA-LED was 30% higher than that of conventional LEDs. The processes attempted on the selective PEC etching process, 22 the controlled wet chemical etching on the AlInN layer, the wet bandgap-selective photoelectrochemical etching process for the liftoff process, <sup>24</sup> and the oxidizing process <sup>25,26</sup> on the GaN materials can also affect the optical properties of nitride-based devices. The crystallographic wet chemical etchings of the p-GaN have

(0001),  $\{10\overline{1}0\}$ , and  $\{10\overline{1}2\}$  stable planes,<sup>27</sup> and the wet chemical etchings of the n-GaN have (0001),  $\{10\overline{1}0\}$ ,  $\{10\overline{1}1\}$ ,  $\{10\overline{1}2\}$ , and  $\{10\overline{1}3\}$  stable planes.<sup>28</sup>

In this article, a description is given on how the continuous cone-shaped-sidewall LED (CSS-LED) structures have been fabricated through a laser scribing process and a selective wet process in hot phosphoric acid (H<sub>3</sub>PO<sub>4</sub>, 170°C for 20 min). This fabrication process consisted of a lateral wet etching process on an AlN buffer layer and a crystallographic etching process on an N-face GaN layer. By forming a stable CSS structure close to the laser scribing lines of the LED chips, the light extraction efficiency of the CSS-LED structure was increased to have a higher light output power and to change the far-field radiation patterns. The relationship between the CSS structure and the light extraction efficiency was analyzed in detail.

#### **Experimental**

InGaN-based LED structures were grown on a polished opticalgrade C-face (0001) 2 in. diam sapphire substrate by using the MOCVD system. Trimethylgallium (TMGa), trimethylaluminum (TMAl), trimethylindium (TMIn), and ammonia (NH<sub>3</sub>) were used as the Ga, Al, In, and N sources, respectively. The doping source gas for the Si, as the donor, was monosilane  $(SiH_4)$  and for Mg as the acceptor, was bis-cyclopentadienylmagnesium (Cp2Mg). These LED structures consisted of a 30 nm thick AlN buffer layer, a 1 µm thick unintentionally doped GaN layer, a 3 µm thick n-type GaN layer, 10 pairs of the InGaN/GaN multiple quantum wells (MOWs) active layers, and a 0.4 µm thick magnesium-doped p-type GaN layer. The active layers consisted of a 30 Å thick InGaN-well layer and a 70 Å thick GaN-barrier layer for the InGaN/GaN MQW LED structures. We cleaved a 2 in. LED wafer into two half-wafers to prepare for this experiment, with a mesa region of  $380 \times 380 \mu m$ LEDs. The LED chips were isolated by using a triple frequency ultraviolet Nd:yttrium aluminum garnet (355 nm) laser for the laser scribing process. The laser scribing depth was  $\sim$ 21.6  $\mu$ m to expose the AlN/sapphire interface for all LED samples shown in Fig. 1b. The dimension of the LED chip was  $420 \times 420 \mu m$  in size, which was defined by the laser scribing process. Half of the LED wafer was immersed in a hot phosphoric acid (H<sub>3</sub>PO<sub>4</sub>, 170°C) for a 20 min crystallographic wet etching process. The wet etching process consisted of a selective lateral etching process on an AlN buffer layer and a bottom-up N-face crystallographic etching process to form the CSS structure around the LED chips. A similar crystallographic etching process to form an inclined undercut LED structure was discussed in detail in our previous report.<sup>29</sup> Next, the n- and p-GaN were defined as the mesa region through the inductively

<sup>&</sup>lt;sup>z</sup> E-mail: cflin@dragon.nchu.edu.tw

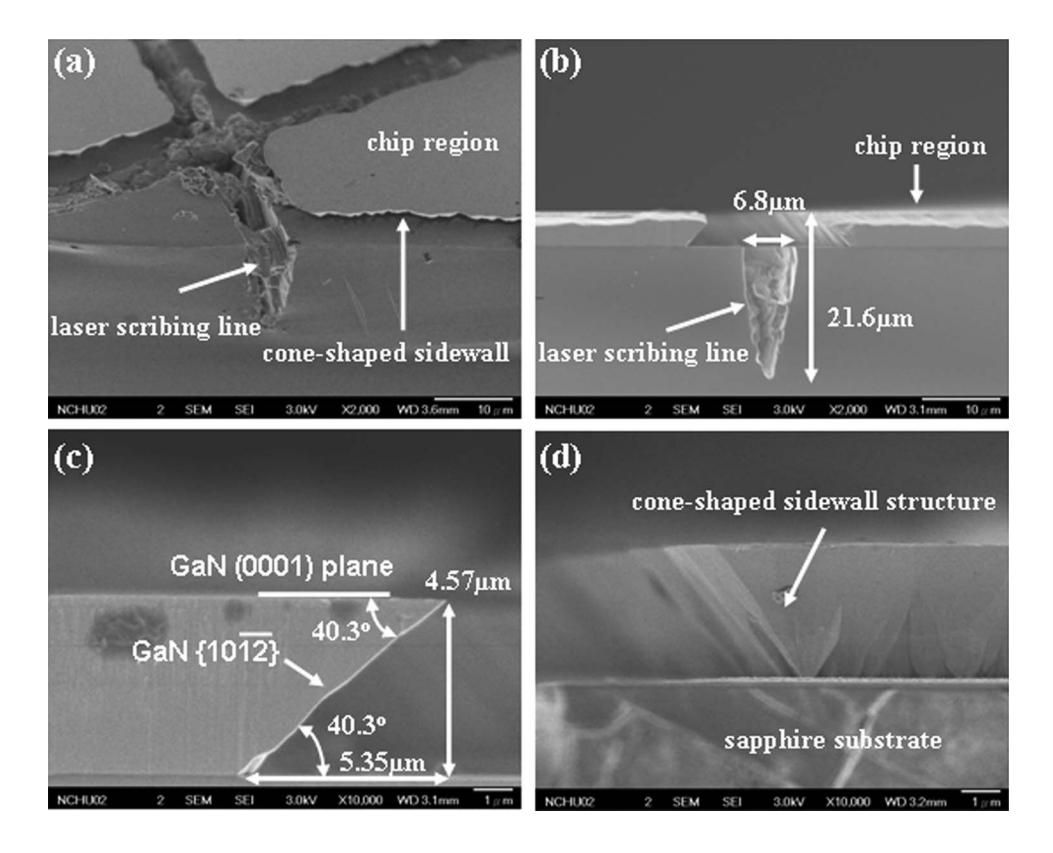


Figure 1. CSS-LED structures are observed in the SEM images. (a) The laser scribing lines between each CSS-LED chip after the wet etching process. (b) The laser cutting width and depth are about 6.8 and 21.6  $\mu m$ , respectively. (c) The CSS structure of the LED is measured at the values of 4.57  $\mu m$  in height and 5.35  $\mu m$  in width. The stable crystallographic etching planes formed at the inclined GaN  $\{101\overline{2}\}$  planes and the top GaN (0001) plane that are both included in the 40.3° angle. (d) The continuous CSS structure close to the laser scribing lines is observed in the CSS-LED structure.

coupled plasma (ICP) etcher using  $\operatorname{Cl}_2$  gas. A 240 nm thick indium tin oxide (ITO) layer was deposited on the mesa region as a transparent contact layer (TCL). The Cr/Au metal layers were deposited as n- and p-type contact pads. The LED device that was fabricated through this process flow without the wet etching process was defined as a standard LED (ST-LED). The LED device that was fabricated by adding the laser scribing process and the crystallographic wet etching process was then defined as a CSS-LED. Both LED structures had laser scribing lines around the LED chips that isolated and separated each of the LED chips. The chosen ST-LED and CSS-LED were both located at the 2 in. LED wafer center near the cleaved line to allow an analysis of the optical and electrical properties from the more similar material properties. The geometric morphology of these LED structures was observed through a scanning electron microscopy (SEM). The optical and electrical properties of both LED samples were measured by using the optical spectrum analyzer and the precision semiconductor parameter analyzer, HP 4156C. The light output power and far-field radiation patterns were measured on nonencapsulated LEDs in chip form. The light intensity profiles that crossed the whole LED samples were measured by a beam profiler (Spiricon: number of effective pixels: 1600  $\times$  1200 pixels).

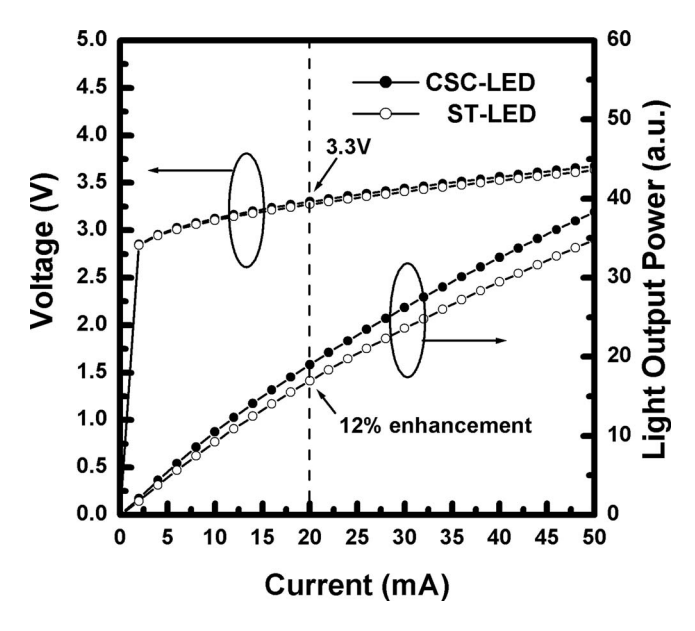
#### Results and Discussion

From the cross-sectional SEM images shown in Fig. 1b, the laser scribing depth on the CSS-LED structure was measured as 21.6  $\mu m$  that isolated the InGaN-based LED chips. The AlN buffer layer was then exposed for the selective lateral wet etching process. After a 20 min crystallographic wet etching process in a hot  $H_3PO_4$  solution, the CSS structures of the LED chips were formed at the LED chip edge region shown in Fig. 1c. The lateral wet etching width from the laser scribing line was  $\sim\!9.17~\mu m$  measured in Fig. 1b and the lateral etching rate of the AlN buffer layer was calculated as 27.5  $\mu m/h$ . The lateral etching process on the AlN buffer layer and the bottom-up N-face crystallographic wet etching process on the GaN-based epitaxial layer were used to form the continuous CSS structures. From the SEM image shown in Fig. 1c, the dimensions of the CSS structure of the CSS-LED were measured as values of

4.57  $\mu$ m in height and 5.35  $\mu$ m in width. The stable crystallographic etching planes were formed as GaN {1012} planes and had an including angle with the top GaN (0001) plane calculated as 40.3°. Stocker et al. <sup>27,28</sup> reported that the GaN epilayers have been crystallographically etched as {1012} planes in H<sub>3</sub>PO<sub>4</sub> at 132°C. The stable and controllable CSS structure was formed when the GaN {1012} plane and top GaN (0001) plane met at the continuous cone-shaped edge. After the laser scribing and crystallographic wet etching process, the continuous CSS structure was observed in the CSS-LED structure shown in Fig. 1d.

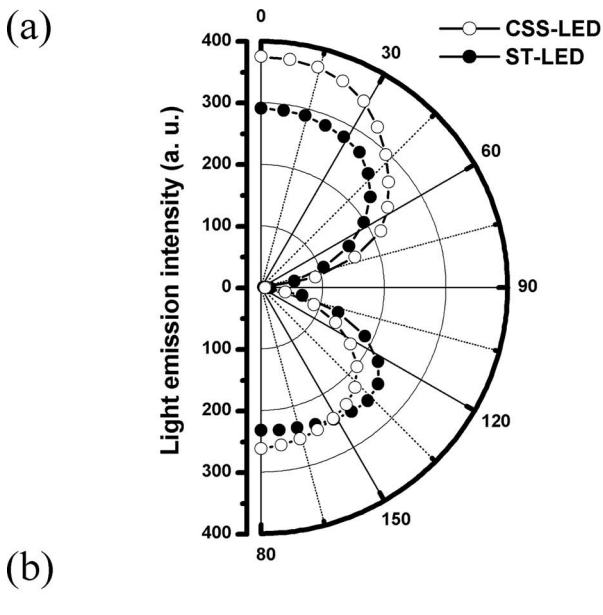
In Fig. 2, the light output power and the operation voltage as functions of the dc injection current were measured. The light output power of the CSS-LED had a 12% enhancement compared with the ST-LED at a 20 mA operating current. The operation voltages of both LED samples were almost the same at the value of 3.3 V at 20 mA. This is because the treated region after the laser scribing and lateral wet etching processes was far from the mesa region and the metal contact regions of the CSS-LED structure.

At 20 mA, the far-field radiation patterns and the light-enhanced ratio of both LED samples were measured from the normal direction  $(\theta = 0^{\circ})$  to the back-side direction  $(\theta = 180^{\circ})$  as seen in Fig. 3a and b. The emission wavelengths of both LEDs were measured at 475 nm with a 25 nm linewidth for the integrated intensity analysis. The radiation pattern for the ST-LED is nearly the same as the Lambertian emission pattern at the front side of an LED chip. The radiation pattern of the CSS-LED is different from the ST-LED in that the light-emission intensity was higher in the front side and was lower in one part of the back side. The light output power at the front side of the LED chip was calculated by summing up the lightemission intensity from 0 to 90° detected angles. The enhanced ratio of light output power at the front side (from  $\theta = 0$  to  $90^{\circ}$ ) and the back side (from  $\theta = 90$  to  $180^{\circ}$ ) were calculated as values of 1.28 and 0.92 times compared to the ST-LED. The total lightenhanced ratio of the CSS-LED was 1.1 times higher compared to the ST-LED when summing up the light-emission intensity from all directions (0-180° detected angles).



**Figure 2.** Light output power and operation voltage as functions of the dc injection current are measured at 20 mA. The light output power of the CSS-LED has a 12% enhancement compared to a ST-LED. The operation voltages are almost the same at 3.3 V.

The light-enhanced ratios as a function of the detected angles are defined as the values of the light-emission intensity of the CSS-LED divided by the ST-LED at each detected angle, as shown in Fig. 3b. The light-enhanced ratio of the CSS-LED has its highest value (1.84) at the lateral direction ( $\sim 86^{\circ}$ ), but its light-emission intensity is lower than the normal direction ( $\theta = 0^{\circ}$ ). At the front side of the LED chip, the higher enhanced ratio (~1.28 times) was observed at the detected range of angles between 0 and 22° and the lowest enhanced ratio (about 1.16 times) was observed at 46°. At the back side of the LED chip, the lower light-emission intensity and lower enhanced ratio (below 1.0 times) were observed at the range of angles between 90 and 136° that might be caused by the total internal reflection that occurs at the inclined  $\{10\overline{12}\}$  stable planes of the CSS-LED structures. Part of the light emitted from the InGaN/GaN MQW active layer was reflected by the inclined {1012} planes to enhance the higher light-emission intensity at the front side of the CSS-LED chip. The CSS-LED structure has stable inclined {1012} planes and CSS structures, resulting in a higher light-extraction efficiency at the range of angles between 152 and 180°. This is because the light-emission cones from the active layer and the lightextraction cones on the inclined  $\{10\overline{12}\}$  planes have a higher overlapping ratio that increases the light-extraction efficiency. The included angle of the inclined {1012} GaN planes and top GaN (0001) plane is 40.3°. Strauss et al.<sup>30</sup> mention that the optimized chip sidewalls have vertical angles of 60° and a 55% higher percentage of light extraction in an ATON structure. This CSS-LED structure consists of inclined  $\{10\overline{12}\}$  stable planes that can increase the light-extraction efficiency in a similar way to the results on a GaNbased LED ATON structure through an SiC-shaping substrate process.<sup>31</sup> Chang et al.<sup>32</sup> reported that the ICP-etched wavelike sidewalls mainly enhance the light output at the horizontal directions. The CSS structure has a larger sidewall surface and a better lightextraction angle on the chip sidewall that permit higher lightextraction efficiency. The light output power of CSS-LED increased at the front side (1.28 times) and decreased at the back side (0.92 times) of the chips. After the chip-sidewall-shaping process, a higher light-extraction efficiency was observed in the CSS-LED structure that increased the external quantum efficiency.



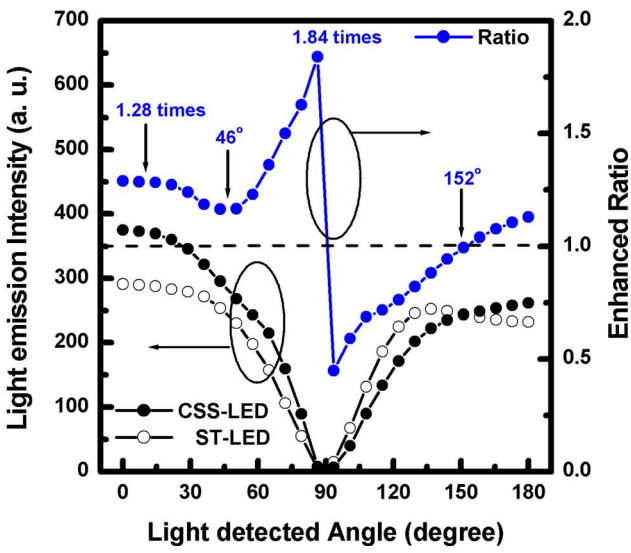


**Figure 3.** (Color online) LED samples show measurements of (a) far-field radiation patterns and (b) light-enhanced ratios from the normal direction  $(\theta=0^\circ)$  to the back-side direction  $(\theta=180^\circ)$ . The light-enhanced ratios as a function of the detected angles are defined as the values of the light-emission intensity of the CSS-LED divided by the ST-LED at each detected angle.

The light intensity profiles of both LED samples at a 20 mA operation current were measured by a beam profiler shown in Fig. 4. The top view and 45° bird's eye view of the light intensity patterns of both LED samples are shown in Fig. 4a-d. In the ST-LED structure, a higher light intensity was observed around the chip edge caused by the light-scattering process from the laser scribing lines. In the CSS-LED structure, a much higher light intensity was observed around the LED chip that has a larger light-scattering process that occurs at the CSS structure close to the laser scribing lines. In both LED structures, the light intensity in the mesa regions on the ITO layer was almost the same. A lower light-intensity region on the ST-LED was observed in the ICP-etched n-type GaN:Si layer.

The schematic diagrams of the CSS InGaN-based LED structures are shown in Fig. 5a. To analyze the light-intensity distribution over the whole LED chips, the line-scanning light-intensity profiles of both LED samples are shown in Fig. 5b, where the observation positions are marked in Fig. 4a and b with dashed lines along the *x*-axis. In Fig. 5a, the regions of the CSS-LED structure were la-

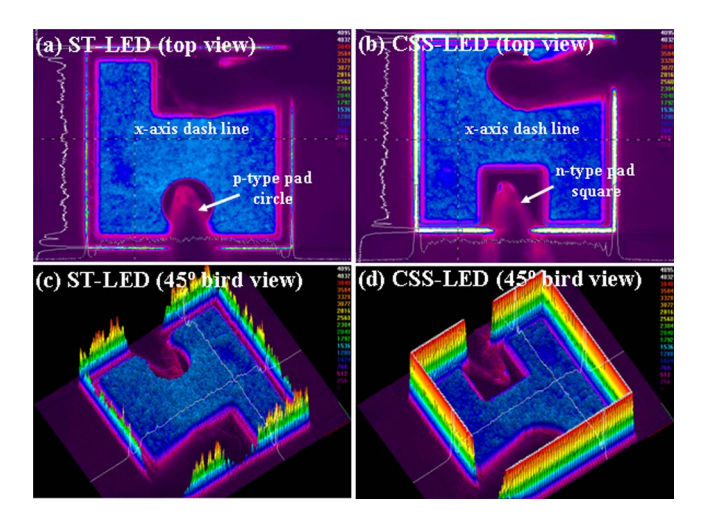
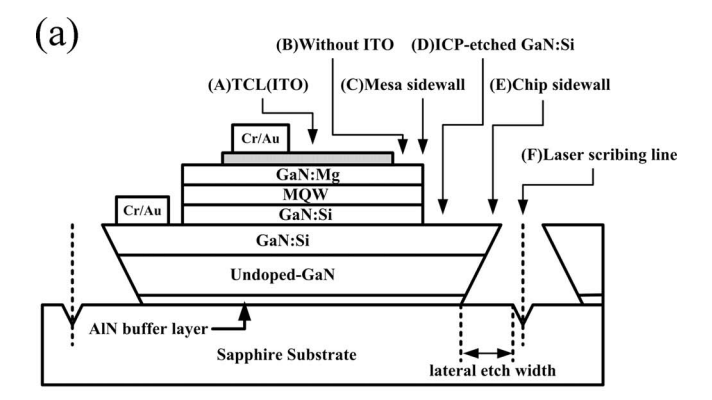


Figure 4. (Color online) Light intensity profiles of both LED samples at a 20 mA operation current are measured by the beam profiler. (a, b) top view and (c, d) 45° bird's eye view of light intensity patterns for both LED samples are observed at a 20 mA operation current.

beled as the TCL region (A), the mesa region without an ITO layer (B), the mesa sidewall (C), the ICP-etched GaN:Si layer (D), the chip sidewall (E), and the laser scribing line (F). From the lightintensity profiles in Fig. 5b, the lower light-intensity regions were observed at the 10 µm width around the mesa edge region without an ITO layer (region B) and an ICP-etched n-type GaN:Si surface close to the laser scribing lines (region D). After the lateral wet etching process on the CSS-LED structure, the higher light-intensity peak was observed at the laser scribing line (region F), the chip sidewall region with the CSS structure (region E), and on part of the n-type GaN:Si layer (region D). The width of the higher intensity region increased in the CSS-LED device caused by the higher lightextraction process and the light-scattering process that occurred at the CSS structures. When the light is generated from the InGaN/GaN active layer, the emission light will propagate to the chip edge region caused by the total internal reflection process that occurred at the top of the GaN/air and the bottom GaN/sapphire interface. Then, the propagated light can be extracted by the continuous CSS structure to increase the external quantum efficiency in the CSS-LED structure. The resolution of the beam profiler is 0.4 µm/pixel, where the width of the LED image is 650 µm and the pixel numbers along the x-axis are 1600 pixels. The widths of the higher light-intensity region (chip sidewall region) close to the laser scribing lines were measured at the values of 9 and 24 µm of the ST-LED and the CSS-LED structures, respectively. The larger emission width and higher light intensity of the CSS-LED were caused by the larger light-scattering process at the laser scribing lines and the higher light-extracting process through the continuous CSS structure. The higher light output power and the different shape of the far-field radiation pattern were measured in the CSS-LED structure that has a higher light-extraction effect around the chip edge region.

### Conclusion

The CSS 1 LED structures were fabricated through a lateral wet etching and a crystallographic wet etching process in a hot H<sub>3</sub>PO<sub>4</sub> solution. The included angle of the crystallographic inclined {1012} GaN planes and top GaN (0001) plane was measured as 40.3°. The higher light intensity of the CSS-LED structure was observed at the chip edge region from a line-scanning light-intensity profile measurement. The chip-sidewall-shaping process with the continuous cone-shaped structures close to the laser scribing lines can increase the light-extraction efficiency of nitride-based LEDs.



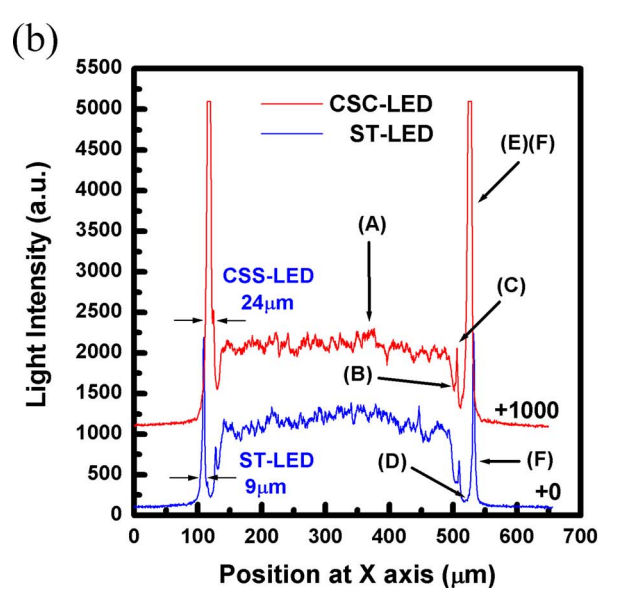


Figure 5. (Color online) (a) Schematic diagram of the CSS InGaN-based LED structure is shown. The regions of the LED structure are labeled as (A) the TCL region. (B) the mesa region without an ITO layer. (C) the mesa sidewall, (D) the ICP-etched GaN:Si layer, (E) the chip sidewall, and (F) the laser scribing lines. (b) The light intensity profiles across the whole LED structures (along the x-axis direction) are measured to analyze the lightemission properties of both LED structures.

## Acknowledgments

The authors gratefully acknowledge the financial support for this research by the National Science Council of Taiwan under grant no. NSC95-2221-E-005-132-MY3, no. NSC96-2622-E-005-004-CC3, no. NSC97-2120-M-009-001, and the Ministry of Economic Affairs under contract no. 97-EC-17-A-07-SI-097. They also acknowledge the technical measurement support from the Unice E-O Services,

National Chung Hsing University assisted in meeting the publication costs of this article.

## References

- 1. W. L. Barnes, J. Lightwave Technol., 17, 2170 (1999).
- B. J. Matterson, J. M. Lupton, A. F. Safonov, M. G. Salt, W. L. Barnes, and I. D. W. Samul, Adv. Mater. (Weinheim, Ger.), 13, 123 (2001).
- H. J. Peng, Y. L. Ho, X. J. Xu, and H. S. Kwok, J. Appl. Phys., 96, 1649,(2004).
- I. Schnitzer, E. Yablonovitch, C. Caneau, T. J. Gmitter, and A. Scherer, Appl. Phys. Lett., 63, 2174 (1993).
- 5. R. Windisch, C. Rooman, S. Meinlschmidt, P. Kiesel, D. Zipperer, G. H. Döhler, B. Dutta, M. Kuijk, G. Borghs, and P. Heremans, Appl. Phys. Lett., 79, 2315 (2001).
- K. Tadatomo, H. Okagawa, Y. Ohuchi, T. Tsunekawa, Y. Imada, M. Kato, and T. Taguchi, *Jpn. J. Appl. Phys., Part* 2, 40, L583 (2001).
  C. Huh, K. S. Lee, E. J. Kang, and S. J. Park, *J. Appl. Phys.*, 93, 9383 (2003).
  S. J. Chang, L. W. Wu, Y. K. Su, Y. P. Hsu, W. C. Lai, J. M. Tsai, J. K. Sheu, and
- C. T. Lee, IEEE Photonics Technol. Lett., 16, 1447 (2004).

- 9. A. David, T. Fujii, R. Sharma, K. Mcgroody, S. Nakamura, S. P. DenBaars, E. L. Hu, and C. Weisbuch, Appl. Phys. Lett., 88, 061124 (2006)
- 10. T. N. Oder, K. H. Kim, J. Y. Lin, and H. X. Jiang, Appl. Phys. Lett., 84, 466 (2004)
- 11. H. K. Cho, J. Jang, J.-H. Choi, J. Choi, J. Kim, J. S. Lee, B. Lee, Y. H. Choe, K.-D.
- Lee, S. H. Kim, et al., Opt. Express, 14, 8654 (2006).

  12. K. Orita, S. Tamura, T. Takizawa, T. Ueda, M. Yuri, S. Takigawa, and D. Ueda,
- Jpn. J. Appl. Phys., Part I, 43, 5809 (2004).
   H. G. Kim, M. G. Na, H. K. Kim, H. Y. Kim, J. H. Ryu, T. V. Cuong, and C.-H. Hong, Appl. Phys. Lett., 90, 261117 (2007).
- 14. C. F. Lin, Z. J. Yang, J. H. Zheng, and J. J. Dai, IEEE Photonics Technol. Lett., 17, 2038 (2005).
- 15. T. Fujii, Y. Gao, R. Sharma, E. L. Hu, S. P. DenBaars, and S. Nakamura, Appl. Phys. Lett., 84, 855 (2004).
- J. Zhong, H. Chen, G. Saraf, Y. Lu, C. K. Choi, J. J. Song, D. M. Mackie, and H. Shen, *Appl. Phys. Lett.*, 90, 203515 (2007).
- 17. M.-K. Lee, C.-L. Ho, and P.-C. Chen, IEEE Photonics Technol. Lett., 20, 252 (2008).
- 18. C. H. Chiu, C. E. Lee, C. L. Chao, B. S. Cheng, H. W. Huang, H. C. Kuo, T. C. Lu, S. C. Wang, W. L. Kuo, C. S. Hsiao, et al., Electrochem. Solid-State Lett., 11, H84 (2008).
- 19. S. S. Schad, T. M. Scherer, M. Seyboth, and V. Schwegler, Phys. Status Solidi A, **188**, 127 (2001).
- 20. J.-S. Lee, J. Lee, S. Kim, and H. Jeon, IEEE Photonics Technol. Lett., 18, 1588 (2006).

- 21. H. G. Kim, T. V. Cuong, M. G. Na, H. K. Kim, H. Y. Kim, J. H. Ryu, and C.-H. Hong, IEEE Photonics Technol. Lett., 20, 1284 (2008).
- 22. E. D. Haberer, R. Sharma, A. R. Stonas, S. Nakamura, S. P. DenBaars, and E. L. Hu, Appl. Phys. Lett., 85, 762 (2004).
- 23. D. Simeonov, E. Feltin, H.-J. Bühlmann, T. Zhu, A. Castiglia, M. Mosca, J.-F. Carlin, R. Butté, and N. Grandjean, Appl. Phys. Lett., 90, 061106 (2007).
- 24. A. R. Stonas, T. Margalith, S. P. DenBaars, L. A. Coldren, and E. L. Hu, Appl. Phys. Lett., 78, 1945 (2001).
- 25. L. H. Peng, C. H. Liao, Y. C. Hsu, C. S. Jong, C. N. Huang, J. K. Ho, C. C. Chiu,
- and C. Y. Chen, *Appl. Phys. Lett.*, **76**, 511 (2000). 26. J. W. Seo, C. S. Oh, H. S. Jeong, J. W. Yang, K. Y. Lim, C. J. Yoon, and H. J. Lee, Appl. Phys. Lett., 81, 1029 (2002).
- 27. D. A. Stocker, I. D. Goepfer, K. S. Boutros, and J. M. Redwing, J. Electrochem. Sec., 147, 763 (2000).
- 28. D. A. Stocker, E. F. Schubert, and J. M. Redwing, Appl. Phys. Lett., 73, 2654 (1998).
- 29. C. F. Lin, Z. J. Yang, J. H. Zheng, and J. J. Dai, J. Electrochem. Soc., 153, G39
- 30. U. Strauss, H. J. Lugauer, A. Weimar, J. Baur, G. Brüderl, D. Eisert, F. Kühn, U. Zehnder, and V. Härle, Phys. Status Solidi C, 0, 276 (2002).
- 31. J. Baur, B. Hahn, M. Fehrer, D. Eisert, W. Stein, A. Plössl, F. Kühn, H. Zull, M.
- Winter, and V. Härle, *Phys. Status Solidi A*, **194**, 399 (2002).
  32. C. S. Chang, S. J. Chang, Y. K. Su, C. T. Lee, Y. C. Lin, W. C. Lai, S. C. Shei, J. C. Ke, and H. M. Lo, *IEEE Photonics Technol. Lett.*, **16**, 750 (2004).